

# $g$ factor of the $12^+$ $K$ -isomer in $^{174}\text{W}$

M. Rocchini<sup>1,2,3</sup>, A. Nannini<sup>1</sup>, G. Benzoni<sup>4,a</sup>, E. Vigezzi<sup>4</sup>, B. Meloni<sup>1</sup>, P.R. John<sup>5,6,7</sup>, S. Bottoni<sup>4,8</sup>, S. Ceruti<sup>4,8</sup>, R. Avigo<sup>4,8</sup>, P. Sona<sup>1</sup>, C.A. Ur<sup>6</sup>, D. Bazzacco<sup>5,6</sup>, N. Blasi<sup>4</sup>, G. Bocchi<sup>4,8</sup>, A. Bracco<sup>4,8</sup>, F. Camera<sup>4,8</sup>, S. Capra<sup>4,8</sup>, F.C.L. Crespi<sup>4,8</sup>, E.R. Gamba<sup>4,8</sup>, G. Georgiev<sup>9</sup>, A. Giaz<sup>4,8</sup>, A. Gottardo<sup>10</sup>, S. Leoni<sup>4,8</sup>, R. Menegazzo<sup>6</sup>, D. Mengoni<sup>5,6</sup>, C. Michelagnoli<sup>11,b</sup>, B. Million<sup>4</sup>, V. Modamio<sup>10</sup>, A.I. Morales<sup>4,8</sup>, D.R. Napoli<sup>10</sup>, M. Ottanelli<sup>1</sup>, L. Pellegrini<sup>4,8</sup>, A. Perego<sup>1,2</sup>, J.J. Valiente-Dobón<sup>10</sup>, and O. Wieland<sup>4</sup>

<sup>1</sup> INFN Sezione di Firenze, IT-50019 Firenze, Italy

<sup>2</sup> Università degli Studi di Firenze, Dipartimento di Fisica e Astronomia, IT-50019 Firenze, Italy

<sup>3</sup> University of Guelph, Department of Physics, N1G2W1 Guelph, Canada

<sup>4</sup> INFN Sezione di Milano, IT-20133 Milano, Italy

<sup>5</sup> Università degli Studi di Padova, Dipartimento di Fisica e Astronomia, IT-35131 Padova, Italy

<sup>6</sup> INFN Sezione di Padova, IT-35131 Padova, Italy

<sup>7</sup> Institut für Kernphysik, Technische Universität Darmstadt, D-64289 Darmstadt, Germany

<sup>8</sup> Università degli Studi di Milano, Dipartimento di Fisica, IT-20133 Milano, Italy

<sup>9</sup> Centre de Sciences Nucléaires et de Sciences de la Matière (CSNSM), F-91405 Orsay, France

<sup>10</sup> INFN Laboratori Nazionali di Legnaro, IT-35020 Padova, Italy

<sup>11</sup> GANIL, F-14076 Caen, France

Received: date / Revised version: date

**Abstract.** The  $g$  factor of the  $12^+$   $K$ -isomer in  $^{174}\text{W}$  has been measured by means of the time-differential perturbed angular distribution technique as  $g(12^+) = +0.304(11)$ . In addition, the half-life of the isomer has been remeasured as  $T_{1/2}(12^+) = 124(8)$  ns, in agreement with the literature value and confirming the anomalous hindrance  $F$  of the  $E2$  transition to the  $10^+$  level of the ground state band with respect to the  $\gamma$ -tunnelling model prediction. The measured  $g$  factor has been compared with estimates based on experimental  $g$  factors from odd-mass isotopes in the same mass region and with Nilsson model calculations. The results establish unique features of the  $12^+$   $K$ -isomer in  $^{174}\text{W}$ , which can possess a non-pure intrinsic configuration and/or can be characterised by values of the intrinsic quadrupole moment  $Q_0$  and the rotational  $g$  factor  $g_R$  significantly different with respect to the majority of  $K$ -isomers at mass  $A \approx 180$ .

**PACS.** 21.10.Ky Electromagnetic moments – 21.10.Tg Lifetimes, widths – 21.10.Re Collective levels – 27.70.+q  $150 \leq A \leq 189$

## 1 Introduction

Isomeric states have historically played a major role in our understanding of the interplay between single-particle and collective properties in nuclear matter [1, 2]. Since their discovery [3, 4], these states have been main characters to establish what nowadays are well-known features of atomic nuclei, such as the spin-orbit coupling, pairing effects and superfluidity in well deformed, rotating isotopes [5, 6]. At present, isomers are exploited to test our comprehension of nuclear structure [7, 8] and are important to investigate how elements are produced in the universe [9]. In addition, they are employed in nuclear medicine [10]. Other fields of application are being explored, for instance, the use of these nuclear states for energy storage [11] and

to realise coherent  $\gamma$ -ray emission [12]. A detailed understanding of the isomer decay properties is crucial for these studies, in particular for isomer manipulation and control.

In the Os–Hf–W isotopes with mass  $A \approx 180$  many high-spin metastable states have been identified, the so-called  $K$ -isomers. These states arise from the approximate conservation of  $K$ , which, for axially deformed nuclei, is the projection of the spin on the symmetry axis: considering a transition of order  $\lambda$  characterised by a variation in  $K$  equal to  $\Delta K$ , selection rules would allow such transition only when  $\lambda > \Delta K$  if  $K$  is a good quantum number. Actually, hindered transitions with  $\lambda < \Delta K$  are possible, with a degree of forbiddance  $\nu = \Delta K - \lambda$ . In order to classify the decay properties of  $K$ -isomers, the hindrance  $F$  and the reduced hindrance  $f_\nu$  are typically used, which are defined as  $F = T_{1/2}/T_{1/2}^W$  (where  $T_{1/2}$  and  $T_{1/2}^W$  are the partial half-life of the transition and the corresponding Weisskopf estimate [1], respectively) and  $f_\nu = F^{1/\nu}$ .

<sup>a</sup> e-mail: giovanna.benzoni@mi.infn.it

<sup>b</sup> Present address: Institut Laue-Langevin, F-38042 Grenoble Cedex, France

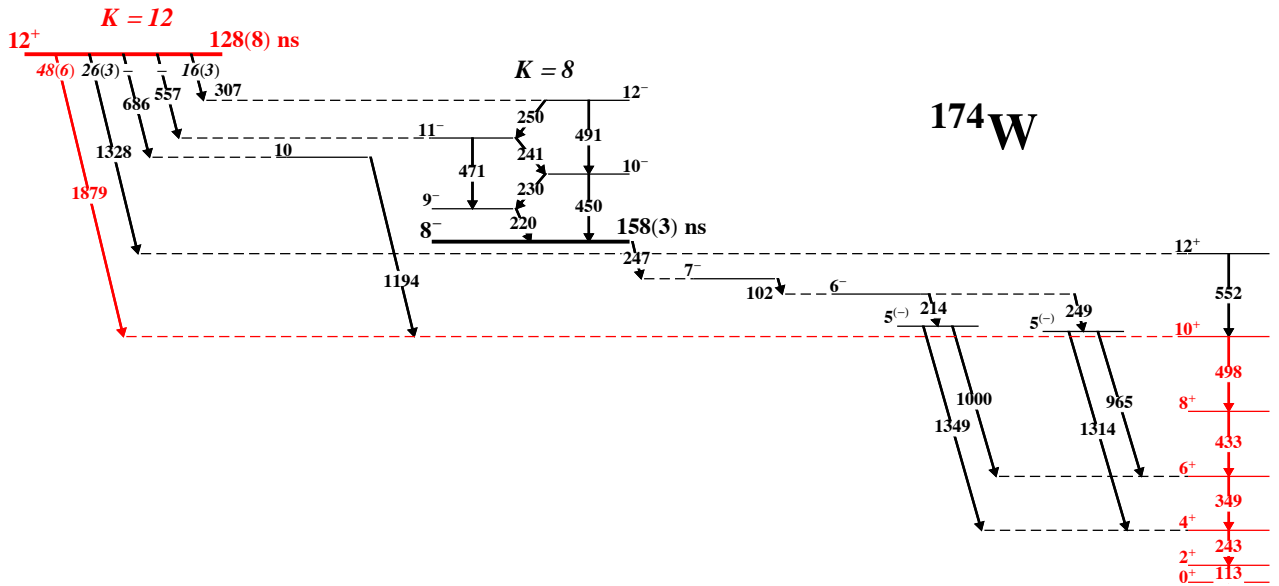


**Fig. 1.** Decay pattern of the  $K = 12^+$  isomer in  $^{174}\text{W}$ . The intensities of the transitions de-exciting the isomer are indicated, given relative to the  $4^+ \rightarrow 2^+$  transition (243 keV) for which the intensity is 10000(300). The  $\gamma$ -cascade of interest for the present work is shown in red. The level scheme and the reported quantities are taken from ref. [18].

Notably, hindered transitions in  $K$ -isomers are commonly characterised by  $f_\nu \approx 30 - 300$ , a relatively narrow range considering that this is valid for the entire nuclide chart [13, 14].

The overall properties of high-spin  $K$ -isomers with predominant decay to the ground state band are often explained as a consequence of the  $\gamma$ -tunnelling mechanism [15–17]. Following this interpretation, the decay is described as a change of the nuclear orientation through a barrier in the  $\gamma$  degree of freedom, along a constant deformation  $\beta$ . Values of  $F$  within an order of magnitude agreement with the measured ones are typically obtained in this model [16, 18], and other second-order effects are implied when the calculated hindrance is larger than the experimental value. The opposite case of smaller calculated  $F$ , instead, indicates that the  $\gamma$ -tunnelling interpretation is totally inappropriate [16] and other mechanisms need to be taken into account, such as shape changes,  $\gamma$  softness, mixing between states with the same  $K$  ( $K$ -mixing) and mixing with states with same spin and parity but different  $K$  (statistical mixing) [15, 19, 20]. Detailed studies have been performed to consider these effects in a few specific cases (see for instance [15, 20]) but a comprehensive and more quantitative description of the  $K$ -isomer decay properties is still missing.

In this context, the  $^{174}\text{W}$  isotope represents an intriguing case. The structure of this nucleus has been investigated in detail using fusion evaporation reactions [18, 21]. Over 300 transitions were observed in ref. [18], allowing to identify 20 rotational bands. Furthermore, a  $I^\pi = 12^+$ ,  $K = 12$  isomer at 3516 keV with  $T_{1/2} = 128(8)$  ns was discovered, characterised by a decay pattern concentrated to the ground state band (see fig. 1). In the same work,  $\gamma$ -tunnelling calculations were performed, obtaining  $F_{calc} = 2.6 \cdot 10^2$  for the most intense transition ( $E2$

to the  $10^+$  state of the ground state band). At variance with other similar  $K$ -isomers in the same mass region, the predicted hindrance is three orders of magnitude lower than the measured one ( $F_{exp} = 7.3 \cdot 10^5$ ) and, therefore, the  $\gamma$ -tunnelling interpretation fails. In a following study, performed by exploiting quasi-continuum  $\gamma$ -spectroscopy techniques, it was concluded that the  $K$ -mixing could be the basic, general phenomenon responsible for the hindrance of the  $\gamma$ -decays in  $^{174}\text{W}$ , both for discrete excited rotational bands and its  $K = 12^+$  isomer [22].

Key information about the structure of  $K$ -isomers can be obtained from magnetic dipole moment measurements [1], which allow for the intrinsic configuration of individual states to be investigated. In order to gain further insights about the anomalous hindrance of the  $K = 12^+$  isomer in  $^{174}\text{W}$ , a dedicated experiment to measure the  $g$  factor of this state was performed.

## 2 Experiment

High-spin states in  $^{174}\text{W}$  were populated in the  $^{162}\text{Dy}(^{16}\text{O}, 4n)^{174}\text{W}$  reaction using a pulsed beam of 84 MeV energy, delivered by the Tandem-XTU at the INFN Legnaro National Laboratories. A repetition cycle of 800 ns was set in between beam bursts of 2 ns duration, allowing to identify a precise time reference and to observe the complete decay of the isomer of interest. The target was composed of a front  $^{162}\text{Dy}$  layer of  $500 \mu\text{g}/\text{cm}^2$  thickness (enriched to 95.1%) and a  $^{nat}\text{Pb}$  thick backing ( $50 \text{ mg}/\text{cm}^2$ ) to stop both the beam and the recoiling  $^{174}\text{W}$  nuclei. The cubic structure of the lead crystalline lattice allowed to keep the nuclear alignment, which was further preserved by heating the whole target to 400 K (the temperature was monitored

with an automatised control system with a sensitivity of 0.5 K).

The same experimental setup exploited in refs. [23–26] for similar  $g$  factor measurements and also quadrupole moment measurements in the same mass region was used. It consists of four coaxial HPGe detectors positioned at  $\pm 45^\circ$  and  $\pm 135^\circ$  with respect to the beam axis. A small vacuum chamber of 10 cm diameter is located at the centre of the array, allowing to position the detectors at a distance of 12 cm from the target. Wax screens of 1 cm thickness were positioned in front of each HPGe, in order to reduce the damage produced by the evaporated neutrons. The setup is equipped with an electromagnet, which was set to provide a 14.65(5) kG magnetic field applied perpendicular to the beam-detector plane, measured by means of a Hall probe. The value of the magnetic field was chosen to allow 2 – 3 complete precessions for transitions de-exciting the  $K = 12^+$  isomer of  $^{174}\text{W}$  in the time range of 3 half-lives<sup>1</sup>. The HPGe detectors were wrapped in  $\mu$ -metal foils in order to avoid distortions in the charge collection efficiency caused by the magnetic field.

Data were acquired using a fast-slow electronic chain. A fast branch was implemented to process signals of the HPGe detectors with a fast-filter amplifier followed by a constant-fraction discriminator, whose output provided the start signal to a time-to-amplitude converter (TAC). The stop signal was given by the delayed beam radiofrequency. In the slow branch, the signal of each HPGe detector was sent to a TNT2 digitizer board [27] to extract the energy information using the moving windows deconvolution method. The output of the TAC was sent to the TNT2 board as well. Once a single HPGe detector provided a trigger, signals from the others were also registered. The event structure was then built off-line, allowing to produce energy and time spectra as well as two-dimensional matrices of energy *vs.* time for each detector. In addition,  $\gamma - \gamma$  matrices were also sorted.

In total, data were collected in 7 days of measurement with an average beam current of 0.3 pA.

### 3 Analysis and results

The half-life of the  $K = 12^+$  isomer in  $^{174}\text{W}$  is well suited for the application the time-differential perturbed angular distribution (TDPAD) technique [28], which exploits the anisotropy of  $\gamma$ -ray emission of an ensemble of oriented nuclei and the Larmor precession that these experience when placed in an external magnetic field. By observing this precession as a function of the time it is possible to measure the associated Larmor frequency, allowing for the  $g$  factor of a specific state to be extracted.

<sup>1</sup> The  $8^-$  level at 2268 keV with  $T_{1/2} = 158(3)$  ns [18] is fed from the the  $K = 12^+$  isomer (see fig. 1). For this reason, and also because of the chosen value of the magnetic field (optimized for the  $K = 12^+$  isomer), the level of statistics achieved in the present experiment prevented the determination of the  $g$  factor for the  $K = 8^-$  isomer.

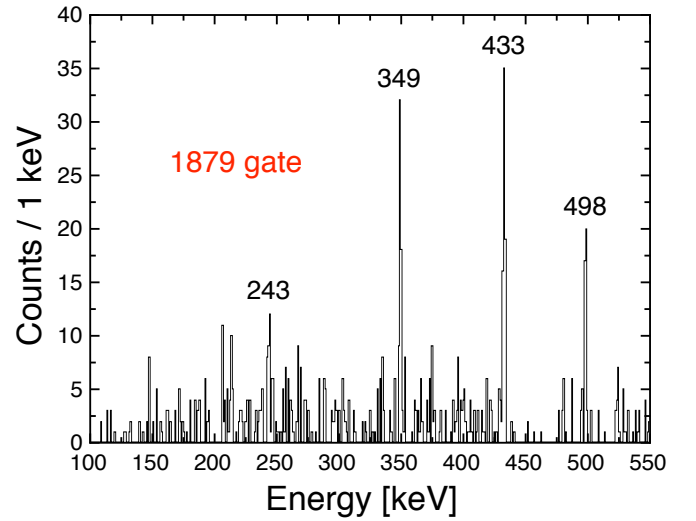


**Fig. 2.** Background-subtracted coincidence spectrum from the total  $\gamma - \gamma$  matrix gated on the  $12^+ \rightarrow 10^+$  transition at 1879 keV, obtained considering events in the delayed time region only. The reduction of statistics for the peaks at 243 keV and 498 keV follows from the  $\gamma$ -ray efficiency of the exploited HPGe array (maximum at  $\approx 400$  keV and rapidly decreasing at  $\approx 250$  keV), which is also the reason why the strongly converted  $2^+ \rightarrow 0^+$  transition at 113 keV is not visible.

High-spin isomers are typically populated with a few per cent of the total cross-section in fusion evaporation reactions (see for instance refs. [23,29]). In the present case, a population of the  $K = 12^+$  isomer of  $\approx 1\%$  was estimated. The decay of this state is concentrated in the  $12^+ \rightarrow 10^+$  transition at 1879 keV, with a  $\gamma$  intensity of 48(6) that represents the 53(8)% of the total de-exciting strength (see fig. 1). In addition, the transitions  $8^+ \rightarrow 6^+$  at 433 keV and  $10^+ \rightarrow 8^+$  at 498 keV were located in a high-background region, identified to be produced by the other delayed transitions from the  $K = 12^+$  isomer (see fig. 1) as well as by long-living nuclei from the  $\beta$ -decay of the reaction products and other neutron-activated materials. For these reasons, only the  $12^+ \rightarrow 10^+$  transition at 1879 keV was clearly visible in the delayed spectra and, therefore, this was the only one considered in the analysis. Other transitions in the ground state band could not be included because they are influenced also by the decay of the other known isomeric state  $8^-$  at 2268 keV, as visible in fig. 1. Figure 2 shows the energy spectrum obtained by gating the total  $\gamma - \gamma$  matrix on the  $12^+ \rightarrow 10^+$  transition, considering the delayed time region only. The expected  $\gamma$ -cascade reported in ref. [18] (shown in fig. 1) is visible.

In order to analyse the data with the TDPAD method, energy spectra were produced off-line by projecting a two-dimensional matrix of energy *vs.* time for each detector, gating on the time every 20 ns starting 40 ns out of the prompt peak (against which time spectra and time axis in the matrices were aligned). The energy peak at 1879 keV was fitted individually in each spectrum and for each detector. The set of obtained values  $I(t, \theta)$  ( $t$  indicates the time interval and  $\theta$  the detector) was then corrected for

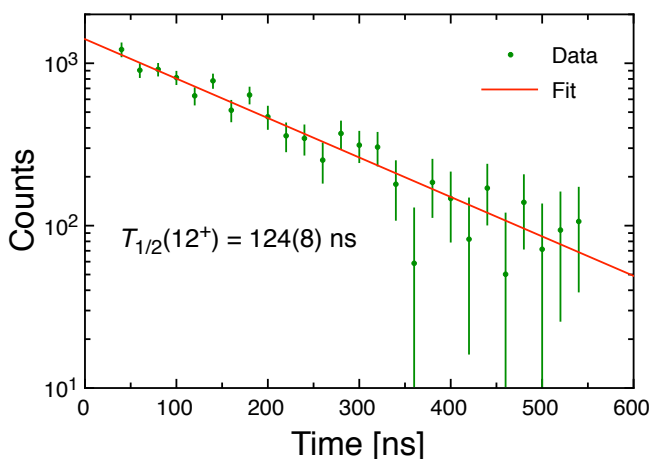


**Fig. 3.** The number of counts measured for the  $12^+ \rightarrow 10^+$  transition at 1879 keV is reported in green as a function of the time. In red, the result of the exponential fit is shown.

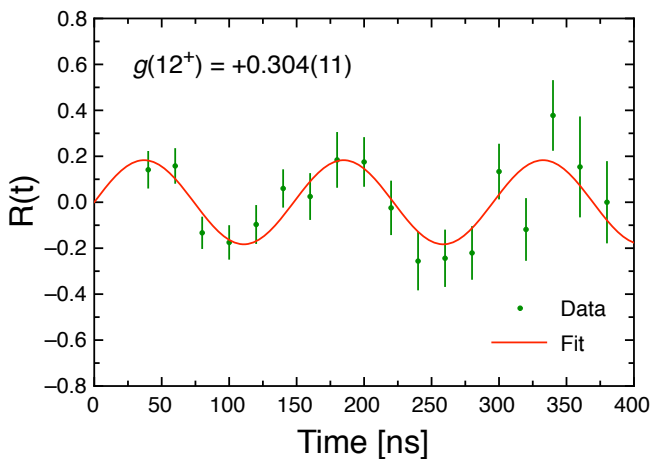


**Fig. 4.** The experimental modulation ratio  $R(t)$  for the  $K = 12^+$  isomeric state in  $^{174}\text{W}$  (obtained considering the  $12^+ \rightarrow 10^+$  transition at 1879 keV) is shown in green, with the result of the least-squares fit in red.

the efficiency of the specific HPGe. The obtained sets of data  $I(t, \theta)$  of detectors positioned at  $180^\circ$  were summed to increase the statistics. Following this, the modulation ratio

$$R(t) = \frac{I^+(t) - I^-(t)}{I^+(t) + I^-(t)} \quad (1)$$

was deduced, where  $I^+(t) = I(t, +45^\circ) + I(t, -135^\circ)$  and  $I^-(t) = I(t, -45^\circ) + I(t, +135^\circ)$ . A different method is more commonly employed to analyse TDPAD data, in which the  $I(t, \theta)$  quantities are directly obtained by projecting the two-dimensional matrices of energy *vs.* time with a gate on the energy, for each detector. After that, the quantity  $R(t)$  is formed as previously explained. Because the transition of interest was relatively weak and it was sitting on a high-background region (the peak-to-background ratio considering the full delayed time range was  $\approx 10\%$ ), this method could not be applied. Indeed,

the fluctuations induced by the background contribution prevailed over the effect of the  $\gamma$  anisotropy. In the present analysis, the exploited method allowed to reduce the statistical error (a comparison and a more detailed description of the two methods can be found in ref. [30]).

The effect of the  $\gamma$  anisotropy can be cancelled by summing the  $I^+(t)$  and  $I^-(t)$  quantities, allowing for the half-life of the isomeric  $12^+$  state to be extracted from the expression  $e^{-t/\tau} \propto I^+(t) + I^-(t)$ . The result of the exponential fit is shown in fig. 3, from which  $T_{1/2}(12^+) = 124(8)$  ns is obtained, in excellent agreement with the literature value (128(8) ns [18]). The amount of data collected in the present experiment precluded the measurement of the half-life of the  $K = 8^-$  isomer of  $^{174}\text{W}$ . Indeed, since the  $K = 12^+$  isomer also decays to this state and the two have comparable half-lives, a double-exponential fit would have been necessary, which required higher statistics than that obtained.

The least-squares fit of the  $R(t)$  ratio was performed by using the expression

$$R(t) = \frac{3A_2B_2}{4 + A_2B_2} \cos[2(\phi - \omega_L t)] \quad (2)$$

from ref. [30], where  $A_2B_2$  and  $\omega_L$  were treated as free parameters. Before the experiment, a new mechanical structure was installed in the exploited setup, which allowed to position the HPGe detectors with a precision of  $0.5^\circ$ . For this reason, the phase  $\phi$  was not considered as a free parameter and it was, instead, fixed to  $45^\circ$  (the systematic uncertainty on this value, as well as the one related to the time alignment, was found to be negligible within the statistical contribution). The result of the least-squares fit procedure is shown in fig. 4. The amplitude of the  $R(t)$  ratio is related to the spin alignment of the isomeric state, which in fusion-evaporation reactions can be described by an oblate Gaussian distribution of  $m$  substates [31]. In this case, the standard deviation of such distribution is typically  $\sigma \approx 0.35I$  [32], where  $I$  is the spin of the excited state. A value of  $A_2B_2 = 0.26(5)$  has been determined in the present analysis, which is consistent with  $\sigma/I = 0.36$ , in excellent agreement with that expected. The  $\omega_L$  parameter is the Larmor frequency, measured as  $\omega_L = 21.3(8)$  MHz, from which

$$g(12^+) = +0.304(11) \quad (3)$$

As visible in fig. 4, no evidence of anisotropy damping has been observed in the present experiment, therefore, more complex fitting parametrisations have not been considered (see ref. [23] for comparison).

## 4 Discussion

As described in refs. [33,34], the measured  $g$  factor allows for the investigation of the quasiparticle configuration of the  $^{174}\text{W}$   $K = 12^+$  isomer. For a state with spin  $I$  and  $K \neq 1/2$ , the  $g$  factor can be decomposed in an intrinsic contribution,  $g_K$  (given by the individual quasiparticles),

and a rotational one,  $g_R$  (resulting from the collective motion of the nucleus), according to eq. 4-87 of ref. [33]:

$$g = g_R + (g_K - g_R) \frac{K^2}{I(I+1)} \quad (4)$$

where  $g \approx g_K$  for  $I = K$  and large values of  $I$ <sup>2</sup>. The quantity  $g_K$  has been firstly calculated by exploiting the same approach followed in ref. [23] to extract the quasiparticle configuration of the  $K = 14^+$  isomer in the close  $^{176}\text{W}$ . In that case, a pure  $2\pi \otimes 2\nu$  configuration was assigned considering  $g_K$  calculated from the experimental  $g$  factors of neighbouring odd-mass nuclei, by using

$$Kg_K = \sum_i \Omega_i g_{\Omega_i} \quad (6)$$

where  $g_{\Omega_i}$  are the intrinsic  $g$  factors obtained from eq. 4 by substituting  $g_K \equiv g_{\Omega_i}$ . It is worth to mention, however, that this approach assumes the same deformation for the isomer and the ground state band in the considered nucleus (in the case of  $^{176}\text{W}$  this assumption was verified in ref. [24]), and that this deformation does not change significantly in the considered neighbouring odd-mass nuclei. The  $g_{\Omega_i}$  values for the orbitals of importance in the present discussion (*i.e.* the ones close to the proton and neutron Fermi surfaces, see refs. [13, 14, 18]) are listed in table 1. From these values, the  $g$  factors for the possible low-lying four quasiparticle configurations of the  $K = 12^+$  isomer have been calculated (see table 2). Because the  $g$  factor depends weakly on the assumed value of  $g_R$ ,  $g_R = 0.25(5)$  has been initially chosen, which represents a typical value measured for several rotational bands in deformed nuclei in the  $A \approx 180$  mass region. The same value was used for similar calculations for the  $K = 14^+$  isomer in  $^{176}\text{W}$  [23], and it was experimentally verified in ref. [24]. As visible in table 2, none of the considered configurations reproduces the experimental  $g(12^+) = 0.304(11)$ . The closest value is calculated for the second  $2\pi \otimes 2\nu$  configuration (*i.e.*  $\pi 5/2^+[402] \otimes \pi 7/2^+[404] \otimes \nu 5/2^+[642] \otimes \nu 7/2^+[633]$ ), for which  $g_{calc} = 0.403(11)$ . The experimental result, therefore, suggests a possible non-pure quasiparticle configuration for the  $K = 12^+$  isomer if  $g_R = 0.25(5)$  and  $g_{\Omega_i}$  values from neighbouring odd-mass nuclei are assumed. In this case, because all the calculated  $g$  factors for  $2\pi \otimes 2\nu$  configurations are above the measured value, the only way to lower the calculated estimate is to include a  $4\nu$  component. For instance, the experimental value could be reproduced by assuming the  $\pi 5/2^+[402] \otimes \pi 7/2^+[404] \otimes \nu 5/2^+[642] \otimes \nu 7/2^+[633]$  configuration of table 2 mixed with 18% of the  $\nu 5/2^+[642] \otimes \nu 7/2^+[633] \otimes \nu 5/2^- [512] \otimes \nu 7/2^- [514]$  configuration or with 23% of the  $\nu 5/2^+[642] \otimes \nu 7/2^+[633] \otimes \nu 5/2^- [523] \otimes \nu 7/2^- [514]$  configuration. A

<sup>2</sup> In the case of a state with  $K = 1/2$ , instead of using eq. 4, the  $g$  factor is calculated with the equation 4-88 of ref. [33]:

$$g = g_R + \frac{g_K - g_R}{4I(I+1)} \left[ 1 + (2I+1)(-1)^{I+\frac{1}{2}} b_0 \right] \quad (5)$$

where  $b_0$  is the magnetic decoupling parameter.

**Table 1.** Values of  $g_{\Omega_i}$  relevant for the present work for  $^{174}\text{W}$ . Column 3 shows  $g_{\Omega_i}$  obtained from  $g$  factors measured in the neighbouring odd-mass nuclei [35], indicated in column 2. The value  $g_R = 0.25(5)$  has been assumed in the calculations (see the text for further information) and the magnetic decoupling parameter  $b_0 = -0.447$  from ref. [36] has been considered for the  $\nu 1/2^- [521]$  state. In column 4,  $g_{\Omega_i}$  values from calculations performed with the Nilsson model considering  $\epsilon = 0.26$  (corresponding to  $Q_0 \approx 7$  eb) are also shown (see the text for further information). Each state is labelled following the usual notation of the Nilsson model  $K^\pi [Nn_z A]$ .

State	$g$ factor [35] Nucleus	$g_{\Omega}$ (exp)	$g_{\Omega}$ (Nilsson)
$\pi 5/2^+[402]$	+1.309(17) $^{181}\text{Ta}, ^{181}\text{Re}$	+1.730(30)	+1.671
$\pi 7/2^+[404]$	+0.649(13) $^{175}\text{Ta}$	+0.763(22)	+0.559
$\pi 9/2^- [514]$	+1.173(20) $^{181}\text{Ta}$	+1.378(27)	+1.348
$\nu 1/2^- [521]$	+0.98734(1) $^{171}\text{Yb}$	+1.570(100)	+1.128
$\nu 5/2^+[642]$	-0.192(1) $^{161}\text{Dy}$	-0.369(20)	-0.346
$\nu 5/2^- [512]$	-0.242(7) $^{175}\text{Hf}$	-0.439(22)	-0.417
$\nu 5/2^- [523]$	+0.249(3) $^{167}\text{Yb}$	+0.249(20)	+0.270
$\nu 7/2^+[633]$	-0.187(6) $^{175}\text{W}$	-0.312(16)	-0.305
$\nu 7/2^- [514]$	+0.227(1) $^{177}\text{Hf}$	+0.220(14)	+0.307

mixed configuration would represent an exception among other similar  $K$ -isomers in the  $A \approx 180$  mass region, where pure configurations are more common. However, it has to be noted that cases of mixed configurations have been already reported in the literature (*e.g.*  $K = 6^+$  isomer in  $^{176}\text{Hf}$  [37] and  $K = 6^+, 8^-$  isomers in  $^{178}\text{Hf}$  [38]). In addition, pure  $4\nu$  configurations have been suggested for a few  $K$ -isomers ( $K = 12^+$  in  $^{178}\text{W}$ ,  $K = 16^+$  in  $^{186}\text{W}$  [13, 14] and  $K = 14^+$  in  $^{174}\text{Yb}$  [39]).

The first two  $2\pi \otimes 2\nu$  configurations considered in table 2 have been also proposed in ref. [18]. Based on the measurement of  $M1/E2$  branching ratios along the band built on the  $K = 12^+$  isomer, the ratio

$$\left| \frac{g_K - g_R}{Q_0} \right| = \frac{1}{K} \sqrt{\frac{5 B(M1) \langle IK20 | I - 2K \rangle^2}{12 B(E2) \langle IK10 | I - 1K \rangle^2}} \quad (7)$$

was determined as  $0.04(1) (\text{eb})^{-1}$  in that work. The first configuration of table 2 (*i.e.*  $\pi 7/2^+[404] \otimes \pi 9/2^- [514] \otimes \nu 1/2^- [521] \otimes \nu 7/2^+[633]$ ) was preferred by the authors, mainly because of the better agreement with the calculated  $|(g_K - g_R)/Q_0|$  ratio, reported in ref. [18] as  $0.05 (\text{eb})^{-1}$  and  $0.004 (\text{eb})^{-1}$  for the first two configurations, respectively. In the same work, calculations based on the cranked Nilsson-Strutinsky framework were performed obtaining total Routhian surfaces, from which a prolate de-

**Table 2.** Possible four-quasiparticle configurations for the  $K = 12^+$  isomer of  $^{174}\text{W}$  and corresponding calculated  $g$  factors and  $|(g_K - g_R)/Q_0|$  ratios. The  $g_{\Omega_i}$  values obtained from  $g$  factors measured in the neighbouring odd-mass nuclei (column 3 in table 1) have been considered. The values  $g_R = 0.25(5)$  and  $Q_0 = 6.96(3)$  eb have been assumed (see the text for further information). Each state is labelled following the usual notation of the Nilsson model  $K^\pi[Nn_zA]$ .

Label	Proton orbitals	Neutron orbitals	$g_{calc}$	$ (g_K - g_R)/Q_0 _{calc}$ [(eb) $^{-1}$ ]
1	$7/2^+[404] \otimes 9/2^-[514]$	$1/2^-[521] \otimes 7/2^+[633]$	+0.678(13)	0.067(7)
2	$5/2^+[402] \otimes 7/2^+[404]$	$5/2^+[642] \otimes 7/2^+[633]$	+0.403(11)	0.024(7)
3	$5/2^+[402] \otimes 7/2^+[404]$	$5/2^-[523] \otimes 7/2^-[514]$	+0.665(11)	0.065(7)
4	$5/2^+[402] \otimes 9/2^-[514]$	$5/2^+[642] \otimes 5/2^-[512]$	+0.674(13)	0.066(7)
5	$5/2^+[402] \otimes 9/2^-[514]$	$5/2^+[642] \otimes 5/2^-[523]$	+0.806(13)	0.087(7)
6	$5/2^+[402] \otimes 7/2^+[404]$	$5/2^-[512] \otimes 7/2^-[514]$	+0.533(11)	0.044(7)
7		$5/2^+[642] \otimes 7/2^+[633] \otimes 5/2^-[512] \otimes 7/2^-[514]$	-0.161(9)	0.064(7)
8		$5/2^+[642] \otimes 7/2^+[633] \otimes 5/2^-[523] \otimes 7/2^-[514]$	-0.029(9)	0.043(7)

formation constant up to  $\hbar\omega = 0.5$  MeV was predicted. From the theoretical  $\beta_2 = 0.271$  value it is possible to deduce  $Q_0 = 6.8$  eb by using the equation  $Q_0 = \frac{3}{\sqrt{5\pi}}ZR^2\beta_2$ , where  $R = 1.2A^{1/3}$ . This value is in agreement with the systematic trend in the neighbouring W isotopes [19], in particular with the value deduced for the  $K = 14^+$  isomer in  $^{176}\text{W}$  ( $Q_0 = 7.37_{-1.01}^{+0.81}$  eb [24]) and with the recent measurement of the lifetime of the first excited  $2^+$  state in  $^{174}\text{W}$ , from which the  $B(E2; 2_1^+ \rightarrow 0_1^+) = 166.9(14)$  W.u. was extracted [40]. Indeed, assuming that the transition quadrupole moment  $Q_t$  is equal to the intrinsic quadrupole moment  $Q_0$  in the ground state band of  $^{174}\text{W}$  (*i.e.* the validity of the rotational model),

$$Q_0 \approx Q_t = \sqrt{\frac{16\pi}{5}} \frac{\sqrt{B(E2; 2_{g.s.}^+ \rightarrow 0_{g.s.}^+)}}{\langle 2020|00 \rangle} \quad (8)$$

A value of  $Q_0 = 6.96(3)$  eb is obtained from eq. 8, close to the predicted  $Q_0 = 6.8$  eb of ref. [18]. Assuming  $Q_0 = 6.96(3)$  eb,  $g_R = 0.25(5)$  and  $g_K$  calculated from experimental  $g$  factors of neighbouring odd-mass nuclei, the  $|(g_K - g_R)/Q_0|$  ratios for the considered four quasiparticle configurations of the  $K = 12^+$  isomer have been recalculated (see table 2). The values obtained for the first two  $2\pi \otimes 2\nu$  configurations differ from the ones reported in ref. [18]. As in the case of the  $g$  factor, the resulting value of  $|(g_K - g_R)/Q_0|$  for the second configuration is closer to the experiment ( $0.04(1)$  (eb) $^{-1}$ ) than for the first one.

The considerations made up to this point about the quasiparticle configuration of the  $K = 12^+$  isomer in  $^{174}\text{W}$  are biased by the choice of  $g_R = 0.25(5)$ . A recent evaluation of this quantity has shown a rather pronounced spreading in its value, which is comprised between  $\approx 0.1 - 0.4$  in the W isotopes [41]. Even if the lowest values are found for the maximum difference between the number of protons and neutrons involved in the quasiparticle configuration ( $N_p - N_n$ ), considerable variations are present also for  $N_p = N_n$ . Therefore, the considered  $g_R = 0.25(5)$  value may not be valid in the present case. Further insights about  $g_R$  for the  $K = 12^+$  isomer can be obtained by combining the experimental  $g$  factor with the  $|(g_K - g_R)/Q_0|$  ratio deduced in ref. [18]. By substituting these two quan-

ties in eqs. 4 and 7 it is possible to find the dependence of  $g_R$  on  $Q_0$  shown in fig. 5, in which both the solutions for  $g_K > g_R$  and  $g_K < g_R$  have been considered<sup>3</sup>. Assuming  $Q_0 = 6.96(3)$  eb for the  $K = 12^+$  isomer, it is possible to obtain  $g_R = 0.56(7)$  and  $g_R = 0.05(7)$  for the two solutions, both far from the adopted  $g_R = 0.25(5)$ . While  $g_R = 0.05(7)$  is compatible with the systematics reported in ref. [41], a value close to  $g_R = 0.56(7)$  has been reported only in ref. [42]. In that work, the  $g_R = 0.59(3)$  value was deduced for the  $6^+$  isomer of  $^{178}\text{Hf}$  combining the measured  $g = 0.970(15)$  with the ratio  $|(g_K - g_R)/Q_0| = 0.0670(25)$  (eb) $^{-1}$ . However, in a following measurement of the  $|(g_K - g_R)/Q_0|$  ratio, a value of  $g_R = 0.35(5)$  was obtained [43]. It is worth to notice how this value is larger than the  $0.25(5)$  estimate and also in agreement with the  $g_R = 0.38(5)$  deduced in ref. [44] for  $^{184}\text{W}$ . Assuming  $g_R = 0.05(7)$ , the calculated  $g$  factors for the  $2\pi \otimes 2\nu$  configurations considered in table 2 decrease by  $\approx 2-4\%$ , while the  $|(g_K - g_R)/Q_0|$  ratios increase by  $\approx 30-120\%$ . For instance, for the second configuration (*i.e.*  $\pi 5/2^+[402] \otimes \pi 7/2^+[404] \otimes \nu 5/2^+[642] \otimes \nu 7/2^+[633]$ )  $g_{calc} = 0.388(12)$  and  $|(g_K - g_R)/Q_0|_{calc} = 0.053(5)$  in this case.

As visible in fig. 5, the value  $g_R = 0.25(5)$  would be compatible with the deduced  $g_R$  dependence on  $Q_0$  if  $Q_0 \leq 4.2$  eb. A reduction of the deformation of the  $K = 12^+$  isomer with respect to the ground state band, or a similar overall deformation but with triaxiality closer to  $\gamma = 30^\circ$ , would be implied in this case. The possibility of having different shapes in  $K$ -isomers with respect to the ground state band as a consequence of different multi-

<sup>3</sup> It should be noted that if the band built on the  $K = 12^+$  isomer is affected by Coriolis mixing, the  $|(g_K - g_R)/Q_0|$  ratio determined from the excited states in the band in ref. [18] could be different than the one of the band head. This would be particularly true if the  $K = 12^+$  isomer configuration includes orbits with  $i_{13/2}$  neutron parentage, such as  $7/2^+[633]$  or  $5/2^+[642]$ . As discussed in ref. [36], the effect of Coriolis interactions could manifest as a renormalization of the  $g_R$  value. However, in the present discussion, it is assumed that the effect of the Coriolis mixing in the band built on the  $K = 12^+$  isomer is negligible and that  $g_R$  is the same in eqs. 4 and 7.

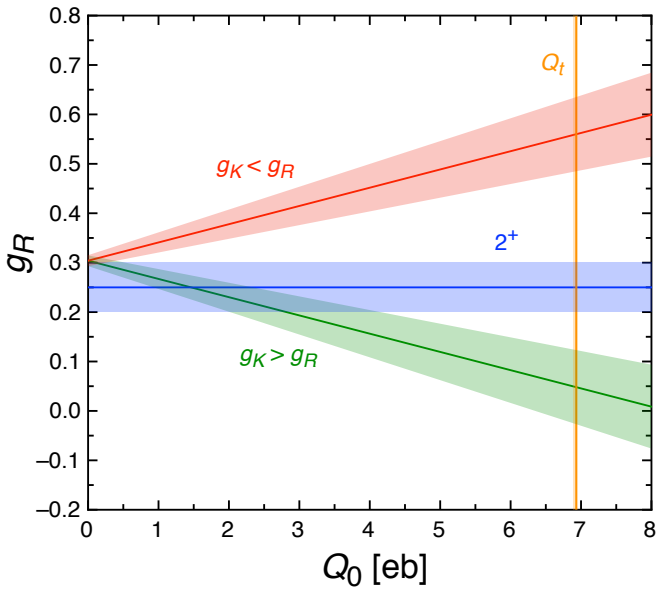


**Fig. 5.** Relation between  $g_R$  and  $Q_0$  for the  $K = 12^+$  isomeric state of  $^{174}\text{W}$ , obtained from the  $g$  factor measured in the present work and the  $|(g_K - g_R)/Q_0|$  ratio deduced in ref. [18]. The solutions with  $g_K > g_R$  and  $g_K < g_R$  are shown in green and red, respectively. The  $g_R$  value resulting from the systematics in other W isotopes is shown in blue. The  $Q_0$  value deduced from the  $B(E2; 2_1^+ \rightarrow 0_1^+)$  measured in ref. [40] is shown in orange ( $Q_0 \approx Q_t$  is assumed). Bands indicate error bars.

quasiparticle configurations was investigated in ref. [15]. In particular, shape polarization effects were found to have significant contributions for particular orbitals. In the case of  $^{182}\text{Os}$ , an anomalously fast decay of the  $K = 25^+$  isomer to the ground state band was found, explained as an effect of  $\gamma$ -softness [45]. An intrinsic quadrupole moment equal to 4.7(2) eb was determined in that case, about 25% lower than the one of the ground state band. Furthermore, in the case of the  $K = 35/2^+$  isomer of  $^{179}\text{W}$  a value of  $Q_0 = 4.73_{-1.25}^{+0.98}$  eb was determined, smaller than that expected for the ground state band [19]. In that case, a significant difference in shape between lower-spin states and the five-quasiparticle isomer was not predicted and a satisfying explanation is still missing in the literature. It is interesting to notice how both the  $Q_0$  values obtained for the  $K = 25^+$  isomer in  $^{182}\text{Os}$  and the  $K = 35/2^+$  isomer of  $^{179}\text{W}$  are close to the  $Q_0 \leq 4.2$  eb limit.

As mentioned at the beginning of this section, if the deformation of the  $K = 12^+$  isomer is substantially smaller than the one of the ground state band (for which  $Q_0 \approx 7$  eb is expected), the  $g_{\Omega_i}$  obtained from the experimental  $g$  factors of the neighbouring odd-mass nuclei may not be valid for the isomer. In order to further investigate the effect of the deformation on the discussed properties, the  $g_{\Omega_i}$  for the relevant orbitals have been also calculated using the Nilsson model. The Nilsson potential parameters have been taken from ref. [46], and the  $g_{\Omega_i}$  values have been evaluated as a function of the deformation parameter  $\epsilon$  with the spin  $g$  factors of both protons and neutrons quenched to 0.8 times the free-nucleon value. The

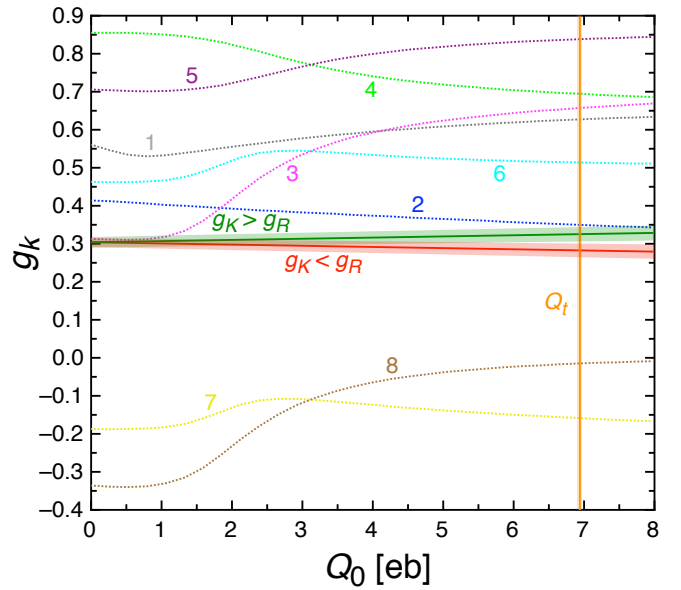


**Fig. 6.** Comparison between experimental  $g_K$  values and the ones calculated for the quasiparticle configurations considered in table 2 as a function of the  $K = 12^+$  isomer deformation. The experimental  $g_K$  has been obtained by using the  $g_R$  dependence on  $Q_0$  shown in fig. 5, *i.e.* by assuming the  $g$  factor measured in the present work and the  $|(g_K - g_R)/Q_0|$  ratio obtained in ref. [18]. The cases  $g_K > g_R$  and  $g_K < g_R$  are shown with green and red continuous lines, respectively. The calculated values have been obtained assuming  $g_{\Omega_i}$  from the Nilsson model as a function of the deformation. The labels indicated in table 2 are used to identify the configurations, shown with dotted lines and different colours. The results are reported as a function of  $Q_0$ , obtained from the  $\epsilon$  deformation parameter of the Nilsson model considering  $Q_0 = \frac{3}{\sqrt{5\pi}}ZR^2\beta_2$  and  $\epsilon \approx 0.95\beta_2$ . The  $Q_0$  value deduced from the  $B(E2; 2_1^+ \rightarrow 0_1^+)$  measured in ref. [40] is shown in orange ( $Q_0 \approx Q_t$  is assumed). Bands indicate error bars.

$g_{\Omega_i}$  values obtained assuming  $\epsilon = 0.26$  (corresponding to  $Q_0 \approx 7$  eb) are shown in table 1, and are in reasonable agreement with the empirical  $g_{\Omega_i}$  values. The  $g$  factors obtained using the Nilsson  $g_{\Omega_i}$  differ from the values reported in table 2 always less than  $\approx 60\%$  (assuming  $g_R = 0.25(5)$ ). From these  $g_{\Omega_i}$  values, the intrinsic  $g$  factors  $g_K$  for the configurations considered in table 2 have been calculated using eq. 6. An empirical estimate of  $g_K$  has been deduced from the  $g_R$  dependence on  $Q_0$  shown in fig. 5 (*i.e.* by assuming the  $g$  factor measured in the present work and the  $|(g_K - g_R)/Q_0|$  ratio obtained in ref. [18]), by exploiting eq. 4. From the comparison of this empirical estimate with the  $g_K$  values calculated with the Nilsson model, shown in fig. 6, it is visible how for the third configuration in table 2 (*i.e.*  $\pi 5/2^+[402] \otimes \pi 7/2^+[404] \otimes \nu 5/2^-[523] \otimes \nu 7/2^-[514]$ ) there is agreement with the experimental  $g_K$  value if  $Q_0 \lesssim 1.1$  eb, both in the case of  $g_K > g_R$  and  $g_K < g_R$ . However, such a small deformation is unprecedented in  $K$ -isomers in the  $A \approx 180$  region of mass, therefore, this solution appears unlikely. The second configuration in table 2 (*i.e.*  $\pi 5/2^+[402] \otimes$

$\pi 7/2^+[404] \otimes \nu 5/2^+[642] \otimes \nu 7/2^+[633]$ ) remain favoured also for smaller values of the deformation. Interestingly, by using the  $g_{\Omega_i}$  values from the Nilsson model, the experimental  $g_K$  in the  $g_K > g_R$  case is in agreement within  $2\sigma$  uncertainty with the value calculated for that configuration if  $Q_0 = 6.96(3)$  eb (see fig. 6). Consequently, in this case also the calculated  $g$  factor  $g_{calc} = 0.326(6)$  is in agreement with the same statistical significance if  $g_R$  is taken from fig. 5, *i.e.*  $g_R = 0.05(7)$  (with the same assumptions, the calculated  $|(g_K - g_R)/Q_0|_{calc} = 0.044(11)$  ratio is in agreement within  $1\sigma$  uncertainty with the value determined in ref. [18]). Considering the other configurations, from fig. 6 it is visible how assuming the  $Q_0 \leq 4.2$  eb limit previously discussed, a  $2\pi \otimes 2\nu$  configuration mixed with a  $4\nu$  one is necessary to reproduce the experimental  $g$  factor obtained in the present work.

## 5 Summary

The  $g$  factor of the  $K = 12^+$  isomer in  $^{174}\text{W}$  has been measured by using the TDPAD technique at the INFN Legnaro National Laboratories. The exploited experimental setup allowed also to remeasure the lifetime of the state, which agrees with the previous measurement [18] and confirms the anomalously large hindrance of the 1879 keV  $E2$  transition with respect to the  $\gamma$ -tunnelling model prediction [18].

From the obtained  $g$  factor, the properties of the  $K = 12^+$  isomer have been further investigated. By combining the value measured in the present work with the ratio  $|(g_K - g_R)/Q_0|$  deduced in ref. [18], the dependence of the rotational  $g$  factor  $g_R$  on the value assumed for the intrinsic quadrupole moment  $Q_0$  has been extracted. From this result, it has been possible to conclude that if the deformation of the  $K = 12^+$  isomer is similar to the one expected for the ground state band in  $^{174}\text{W}$  (for which  $Q_0 \approx 7$  eb),  $g_R$  is significantly smaller than that commonly assumed in the  $A \approx 180$  mass region, *i.e.*  $g_R \approx 0.25$ . Instead, if  $g_R$  is close to this value,  $Q_0$  is smaller in the isomer than in the ground state band. The four quasiparticle configuration of the  $K = 12^+$  isomer has been discussed by comparing the value measured in the present work with estimates based on experimental  $g$  factors of neighbouring odd-mass nuclei and Nilsson model calculations.

From the present analysis, it is concluded that the only candidate for an almost pure  $2\pi \otimes 2\nu$  configuration is the  $\pi 5/2^+[402] \otimes \pi 7/2^+[404] \otimes \nu 5/2^+[642] \otimes \nu 7/2^+[633]$  one, and only if  $g_R \approx 0 - 0.15$  and  $Q_0 \approx 7$  eb for the isomer. For all the other considered configurations and values of  $g_R$  and  $Q_0$ , a  $2\pi \otimes 2\nu$  configuration mixed with a  $4\nu$  one is necessary to reproduce the experimental finding.

In conclusion, unique features seem to emerge from the present results in  $^{174}\text{W}$ , which call for further experimental and theoretical studies. In particular, the measurement of the spectroscopic quadrupole moment  $Q_s$  of the  $K = 12^+$  isomer would allow to establish the deformation of the state and to determine the value of  $g_R$  when combined with the present results. Transitional and diagonal

$E2$  matrix elements in the  $^{174}\text{W}$  ground state band are important as well in order to obtain information about the deformation of this isotope. The effect of Coriolis mixing in the band built on the  $K = 12^+$  isomer should be further investigated. Finally, new calculations of  $\gamma$  tunnelling taking into account the multi-quasiparticle configurations suggested here and the possible reduction of the overall deformation in the  $K = 12^+$  isomer would provide useful insight.

We thankfully acknowledge the staff of the LNL Tandem-XTU accelerator for the high quality of the delivered  $^{16}\text{O}$  beam, M. Loriggiola for producing the target and the mechanical workshops of the INFN division of Florence for their crucial contribution. The contribution of A. Stuchbery in producing table 1 and fig. 6 is gratefully acknowledged. We are also grateful to M. Ionescu-Bujor and P.M. Walker for the fruitful discussions on both the data analysis and the interpretation.

## References

1. G.D. Dracoulis, P.M. Walker and F.G. Kondev, Rep. Prog. Phys. **79**, 076301 (2016).
2. P.M. Walker and G.D. Dracoulis, Nature **399**, 35 (1999).
3. O. Hahn, Chem. Ber. **54**, 1131 (1921).
4. G. Gamow, Phys. Rev. **45**, 728 (1934).
5. A. Bohr and B.R. Mottelson, K. Dan. Vidensk. Selsk. Mat. Fys. Medd. **30**, 1 (1955).
6. M. Goldhaber and R.D. Hill, Rev. Mod. Phys. **24**, 179 (1952).
7. C. Lizarazo *et al.*, Phys. Rev. Lett. **124**, 222501 (2020).
8. S. Leoni *et al.*, Phys. Rev. Lett. **118**, 162502 (2017).
9. A. Aprahamian, K. Langanke and M. Wiescher, Prog. Part. Nucl. Phys. **54**, 535 (2005).
10. C.S. Cutler, H.M. Hennkens, N. Sisay, S. Huclier-Markai and S.S. Jurisson, Chem. Rev. **113**, 858 (2013).
11. K.W.D. Ledingham, P. McKenna and R.P. Singhal, Science **300**, 1107 (2003).
12. L. Marmugi, P.M. Walker and F. Renzoni, Phys. Lett. B **777**, 281 (2018).
13. F.G. Kondev, G.D. Dracoulis and T. Kibédi, At. Data Nucl. Data Tables **1034**, 50 (2015).
14. F.G. Kondev, G.D. Dracoulis and T. Kibédi, At. Data Nucl. Data Tables **1056**, 105 (2015).
15. F.R. Xu, P.M. Walker, J.A. Sheikh and R. Wyss, Phys. Lett. B **435**, 257 (1998).
16. K. Narimatsu, Y.R. Shimizu and T. Shizuma, Nucl. Phys. A **601**, 69 (1996).
17. T. Bengtsson, R.A. Broglia, E. Vigezzi, F. Barranco, F. Dönau and Jing-ye Zhang, Phys. Rev. Lett. **62**, 2448 (1989).
18. S.K. Tandel *et al.*, Phys. Rev. C **73**, 044306 (2006).
19. D.L. Balabanski *et al.*, Phys. Rev. Lett. **86**, 604 (2001).
20. P.M. Walker *et al.*, Phys. Lett. B **408**, 42 (1997).
21. G.D. Dracoulis, P.M. Walker and A. Johnston, J. Phys. G: Nucl. Phys. **4**, 713 (1978).
22. V. Vandone *et al.*, Phys. Rev. C **88**, 034312 (2013).
23. M. Ionescu-Bujor *et al.*, Phys. Lett. B **495**, 289 (2000).
24. M. Ionescu-Bujor *et al.*, Phys. Lett. B **541**, 219 (2002).
25. M. Ionescu-Bujor *et al.*, Phys. Lett. B **650**, 141 (2007).



26. M. Ionescu-Bujor *et al.*, Phys. Rev. C **81**, 024323 (2010).
27. L. Arnold *et al.*, IEEE Trans. Nucl. Sci. **53**, 723 (2006).
28. E. Recknagel, *Nuclear Spectroscopy and Reactions* (J. Cerny, New York, 1974).
29. B. Crowell *et al.*, Phys. Rev. C **53**, 1173 (1996).
30. G. Georgiev, PhD thesis, Department of Physics, University of Leuven (2001).
31. T. Yamazaki, Nucl. Data Sheets Sec. A **3**, 1 (1967).
32. T.J. Gray *et al.*, Phys. Rev. C **101**, 054302 (2020).
33. A. Bohr and B.R. Mottelson, *Nuclear Structure vol. 2*, (World Scientific, Singapore, 1975).
34. F. Boehm *et al.*, Phys. Rev. Lett. **22**, 627 (1966).
35. N.J. Stone, At. Data Nucl. Data Tables **90**, 75 (2005).
36. A.E. Stuchbery, S.S. Anderssen and H.H. Bolotin, Nucl. Phys. A **669**, 27 (2000).
37. P.M. Walker, D. Ward, O. Häusser, H.R. Andrews and T. Faestermann, Nucl. Phys. A **349**, 1 (1980).
38. T.L. Khoo and G. Løvholden, Phys. Lett. B **67**, 271 (1977).
39. G.D. Dracoulis *et al.*, Phys. Rev. C **71**, 044326 (2005).
40. V. Werner *et al.*, Phys. Rev. C **93**, 034323 (2016).
41. N.J. Stone, J.R. Stone, P.M. Walker and C.R. Bingham, Phys. Lett. B **726**, 675 (2013).
42. T. Faestermann *et al.*, Hyperfine Interactions **4**, 216 (1978).
43. S.M. Mullins *et al.*, Phys. Lett. B **393**, 279 (1997).
44. G. Manning and J. Rogers, Nucl. Phys. **19**, 675 (1960).
45. C. Broude *et al.*, Phys. Lett. B **264**, 17 (1991).
46. T. Bengtsson and I. Ragnarsson, Nucl. Phys. A **436**, 14 (1985).